

Presentazione





Questo documento è la versione compilata di un modello \LaTeX di tesi di laurea o di dottorato, pronto all'uso, particolarmente indicato per lavori di carattere scientifico. Basato sul modello di Tesi Moderna proposto da Lorenzo Pantieri, è stato sviluppato per la stesura di tesi di laurea magistrale presso la Scuola di Ingegneria Industriale e dell'Informazione del Politecnico di Milano (PoliMi); esso risulta quindi immediatamente utilizzabile per tesi di Ingegneria al Politecnico di Milano, ma può essere impiegato con le opportune modifiche di layout anche in altre università. L'impianto \LaTeX del modello di tesi (cartelle, files sorgente .tex, esempi di grafici e di database bibliografico) può essere scaricato al link indicato al termine di questa breve presentazione.

Agli Studenti del PoliMi

Le impostazioni di impaginazione sono state scelte con riferimento alle norme di stesura indicate dalla Facoltà di Ingegneria Industriale del Politecnico di Milano. Alcuni di questi parametri sono stati poi sostituiti o modificati per ottenere una resa tipografica più soddisfacente, senza allontanarsi però dalle principali linee guida indicate dal PoliMi; le impostazioni modificate possono essere facilmente ripristinate commentando/decommentando le relative righe di codice dei files sorgente.

Il frontespizio della prima pagina è stato creato con il pacchetto *frontespizio* e (purtroppo) non è quello ufficialmente previsto dal PoliMi. Il frontespizio “a norma” è quello che segue questa presentazione, e che apre inoltre il vero e proprio documento di tesi.

Nelle impostazioni iniziali vengono definiti i quattro colori ricorrenti del PoliMi, presenti anche nel tema delle presentazioni PowerPoint utilizzato dai docenti, che possono essere impiegati arbitrariamente all'interno del testo. Essi sono:

darkbluePoliMi	
midbluePoliMi	
lightbluePoliMi	
orangePoliMi	

A Tutti

Nel modello di tesi proposto i filetti delle tabelle e delle note a piè di pagina sono colorati in `darkbluePoliMi`, come visibile nella tabella sopra; lo scopo è quello di richiamare l'appartenenza all'università con finzze tipografiche che compariranno saltuariamente all'interno del testo. É estremamente semplice annullare questa

modifica all'interno del file ImpostazioniTesi.tex, o cambiare a piacimento il colore utilizzato (ad esempio gli studenti della Sapienza possono usare il **Rosso Sapienza**). A partire dai Link Utili tutto il testo colorato, all'interno del documento, è cliccabile.

Link Utili

Modello di tesi L^AT_EX completo e pronto all'uso:

[link-modello-tesi-latex](#)

Modello di Presentazione Powerpoint per Tesi di Laurea al Politecnico di Milano:

[www.scribd.com](#)

Script Matlab per inizializzare l'ambiente di lavoro e impostare le proprietà delle figure ottimali per la successiva inclusione nell'elaborato della Tesi e nella presentazione PowerPoint:

[www.scribd.com](#)

Mail – per segnalazioni, proposte e suggerimenti:

[inviami-una-email](#)

Materiale L^AT_EX sul sito web personale di Lorenzo Pantieri:

[www.lorenzopantieri.net](#)

Sito web del GuIT – Gruppo Utilizzatori Italiani di T_EX e L^AT_EX:

[www.guitex.org](#)

Politecnico di Milano:

[www.polimi.it](#)

TedOC – Servizio tesi e documentazione del Politecnico di Milano:

[www.tedoc.polimi.it](#)

POLITesi – Archivio digitale delle tesi di laurea e di dottorato del PoliMi:

[www.politesi.polimi.it](#)

POLITECNICO DI MILANO

Scuola di Ingegneria Industriale e dell'Informazione

Corso di Laurea Magistrale in
Ingegneria Meccanica



Modello di Tesi di Laurea in LaTeX

Relatore: Prof. Charles DICKENS

Correlatore: Ing. Emilio SALGARI

Tesi di Laurea di:

Luca MAGGIORI

Matr. 783186

Anno Accademico 2012 - 2013

Luca Maggiori: *Modello di Tesi di Laurea in L^AT_EX* | Tesi di Laurea Magistrale in
Ingegneria Meccanica, Politecnico di Milano.

© Copyright Aprile 2014.

Politecnico di Milano:

www.polimi.it

Scuola di Ingegneria Industriale e dell'Informazione:

www.ingindinf.polimi.it

Ringraziamenti

Lorem ipsum dolor sit amet, consectetur adipiscing elit. Ut purus elit, vestibulum ut, placerat ac, adipiscing vitae, felis. Curabitur dictum gravida mauris. Nam arcu libero, nonummy eget, consectetur id, vulputate a, magna. Donec vehicula augue eu neque. Pellentesque habitant morbi tristique senectus et netus et malesuada fames ac turpis egestas. Mauris ut leo. Cras viverra metus rhoncus sem. Nulla et lectus vestibulum urna fringilla ultrices. Phasellus eu tellus sit amet tortor gravida placerat. Integer sapien est, iaculis in, pretium quis, viverra ac, nunc. Praesent eget sem vel leo ultrices bibendum. Aenean faucibus. Morbi dolor nulla, malesuada eu, pulvinar at, mollis ac, nulla. Curabitur auctor semper nulla. Donec varius orci eget risus. Duis nibh mi, congue eu, accumsan eleifend, sagittis quis, diam. Duis eget orci sit amet orci dignissim rutrum.

Desidero inoltre ringraziare esplicitamente:

Esplicito1 per vari motivi;

Esplicito2 per altri motivi;

Esplicito3 per puro piacere, senza particolari motivi.

Milano, Aprile 2014

L. M.

*a te,
ovunque tu sia,
e qualunque percorso di vita tu abbia intrapreso.*

Indice

Introduzione	1
1 Focusing for X-rays	5
1.1 Introduction	5
1.2 Interaction with Matter	6
1.3 Total External Reflection	9
1.4 Enhancement of Reflectivity	11
2 Mirrors for X-rays	13
2.1 Conic Surfaces	14
2.2 Compound Optical system	15
2.2.1 Sine Abbe condition	15
2.2.2 Wolter System	15
2.2.3 Kirkpatrick-Baez System	16
3 Montel System	17
3.0.1 Optical Design	17
4 Mt script	19
4.1 Source	19
4.2 Optical Elements	19
4.2.1 Mirrors	20
4.2.2 Lens	20
4.3 Tracing System	20
4.4 Compound Optical Element	21
4.4.1 KirkPatrickBaez System	21
4.4.2 Montel System	22
4.5 Tracing system for compound optical elements	22
4.5.1 Tracing for KB	22
4.5.2 Tracing for Montel	23
5 Results	25
5.1 Testing with OASYS	25
5.2 Testing with the paper	25
5.3 Analysis of Montel system	27
5.4 Alignment	27
5.4.1 Orthogonality	28

5.4.2	Incidence angle	29
5.4.3	point of incidence	29
6	Prove Sperimentali	31
6.1	Sezione	31
6.1.1	Subsection	31
7	Analisi Numeriche	35
7.1	Vettori	36
	Conclusioni	37
A	Primo Capitolo d'Appendice	39
A.1	Codici in Linea	39
A.2	Codici in Display e Codici Mobili	39
B	Secondo Capitolo d'Appendice	43
	Acronimi	45

Elenco delle figure

1	Esempi di pantografi.	1
2	Nessuna immagine... Sorry.	2
5.1	Illustration of the Montel system used as a collimator in the paper [RKM15]	26
5.2	Results of the Montel system of a source beam with a FWHM spot of $2.5\mu\text{m}$ and a Gaussian divergence of 5mrad	26
5.3	Results of my Montel simulation of a source beam with a FWHM spot of $2.5\mu\text{m}$ and a Gaussian divergence of 5mrad	27
5.4	Nessuna immagine... Sorry.	28
5.5	Nessuna immagine... Sorry.	28
5.6	Different path for simulate the non-centred beam	29
5.7	Results of the Montel system of a source beam with a FWHM spot of $2.5\mu\text{m}$ and a Gaussian divergence of 5mrad	30
6.1	Esempio di grafici	32

Elenco delle tabelle

2.1	Parameter of different conic surfaces	15
6.1	Principali caratteristiche della camera di prova utilizzata.	31
B.1	Elenco completo delle prove sperimentali	44

Elenco dei codici

A.1	Inizializzazione di MatLab	39
A.2	prova	40
A.3	prova codice intero	40

Sommario

Lorem ipsum dolor sit amet, consectetur adipiscing elit. Ut purus elit, vestibulum ut, placerat ac, adipiscing vitae, felis. Curabitur dictum gravida mauris. Nam arcu libero, nonummy eget, consectetur id, vulputate a, magna. Donec vehicula augue eu neque. Pellentesque habitant morbi tristique senectus et netus et malesuada fames ac turpis egestas. Mauris ut leo. Cras viverra metus rhoncus sem. Nulla et lectus vestibulum urna fringilla ultrices. Phasellus eu tellus sit amet tortor gravida placerat. Integer sapien est, iaculis in, pretium quis, viverra ac, nunc. Praesent eget sem vel leo ultrices bibendum. Aenean faucibus. Morbi dolor nulla, malesuada eu, pulvinar at, mollis ac, nulla. Curabitur auctor semper nulla. Donec varius orci eget risus. Duis nibh mi, congue eu, accumsan eleifend, sagittis quis, diam. Duis eget orci sit amet orci dignissim rutrum.

Nam dui ligula, fringilla a, euismod sodales, sollicitudin vel, wisi. Morbi auctor lorem non justo. Nam lacus libero, pretium at, lobortis vitae, ultricies et, tellus. Donec aliquet, tortor sed accumsan bibendum, erat ligula aliquet magna, vitae ornare odio metus a mi. Morbi ac orci et nisl hendrerit mollis. Suspendisse ut massa. Cras nec ante. Pellentesque a nulla. Cum sociis natoque penatibus et magnis dis parturient montes, nascetur ridiculus mus. Aliquam tincidunt urna. Nulla ullamcorper vestibulum turpis. Pellentesque cursus luctus mauris.

Parole chiave: PoliMi, Tesi, LaTeX, Scribd

Abstract

Text of the abstract in english...

Lorem ipsum dolor sit amet, consectetur adipiscing elit. Ut purus elit, vestibulum ut, placerat ac, adipiscing vitae, felis. Curabitur dictum gravida mauris. Nam arcu libero, nonummy eget, consectetur id, vulputate a, magna. Donec vehicula augue eu neque. Pellentesque habitant morbi tristique senectus et netus et malesuada fames ac turpis egestas. Mauris ut leo. Cras viverra metus rhoncus sem. Nulla et lectus vestibulum urna fringilla ultrices. Phasellus eu tellus sit amet tortor gravida placerat. Integer sapien est, iaculis in, pretium quis, viverra ac, nunc. Praesent eget sem vel leo ultrices bibendum. Aenean faucibus. Morbi dolor nulla, malesuada eu, pulvinar at, mollis ac, nulla. Curabitur auctor semper nulla. Donec varius orci eget risus. Duis nibh mi, congue eu, accumsan eleifend, sagittis quis, diam. Duis eget orci sit amet orci dignissim rutrum.

Nam dui ligula, fringilla a, euismod sodales, sollicitudin vel, wisi. Morbi auctor lorem non justo. Nam lacus libero, pretium at, lobortis vitae, ultricies et, tellus. Donec aliquet, tortor sed accumsan bibendum, erat ligula aliquet magna, vitae ornare odio metus a mi. Morbi ac orci et nisl hendrerit mollis. Suspendisse ut massa. Cras nec ante. Pellentesque a nulla. Cum sociis natoque penatibus et magnis dis parturient montes, nascetur ridiculus mus. Aliquam tincidunt urna. Nulla ullamcorper vestibulum turpis. Pellentesque cursus luctus mauris.

Keywords: PoliMi, Master Thesis, LaTeX, Scribd

Introduzione

Due esempi di pantografi in presa sono mostrati in figura 1; l'architettura asimmetrica del quadro (1b) è quella tradizionalmente adottata per i pantografi impiegati nell'alta velocità ferroviaria.

Argomento da Approfondire¹

Qualche citazione. Lorem ipsum dolor sit amet, consectetur adipiscing elit. Ut purus elit, vestibulum ut, placerat ac, adipiscing vitae, felis. Curabitur dictum gravida mauris. Nam arcu libero, nonummy eget, consectetur id, vulputate a, magna. Donec vehicula augue eu neque. Pellentesque habitant morbi tristique senectus et netus et malesuada fames ac turpis egestas. Mauris ut leo. Cras viverra metus rhoncus sem. Nulla et lectus vestibulum urna fringilla ultrices. Phasellus eu tellus sit amet tortor gravida placerat. Integer sapien est, iaculis in, pretium quis, viverra ac, nunc. Praesent eget sem vel leo ultrices bibendum. Aenean faucibus. Morbi dolor nulla, malesuada eu, pulvinar at, mollis ac, nulla. Curabitur auctor semper nulla. Donec varius orci eget risus. Duis nibh mi, congue eu, accumsan eleifend, sagittis quis, diam. Duis eget orci sit amet orci dignissim rutrum.

Nam dui ligula, fringilla a, euismod sodales, sollicitudin vel, wisi. Morbi auctor lorem non justo. Nam lacus libero, pretium at, lobortis vitae, ultricies et, tellus. Donec aliquet, tortor sed accumsan bibendum, erat ligula aliquet magna, vitae ornare odio metus a mi. Morbi ac orci et nisl hendrerit mollis. Suspendisse ut massa. Cras nec ante. Pellentesque a nulla. Cum sociis natoque penatibus et magnis dis parturient montes, nascetur ridiculus mus. Aliquam tincidunt urna. Nulla ullamcorper vestibulum turpis. Pellentesque cursus luctus mauris.



(a) Architettura simmetrica



(b) Architettura asimmetrica

Figura 1: Esempi di pantografi.



Figura 2: Nessuna immagine. . . Sorry.

Nulla malesuada porttitor diam. Donec felis erat, congue non, volutpat at, tincidunt tristique, libero. Vivamus viverra fermentum felis. Donec nonummy pellentesque ante. Phasellus adipiscing semper elit. Proin fermentum massa ac quam. Sed diam turpis, molestie vitae, placerat a, molestie nec, leo. Maecenas lacinia. Nam ipsum ligula, eleifend at, accumsan nec, suscipit a, ipsum. Morbi blandit ligula feugiat magna. Nunc eleifend consequat lorem. Sed lacinia nulla vitae enim. Pellentesque tincidunt purus vel magna. Integer non enim. Praesent euismod nunc eu purus. Donec bibendum quam in tellus. Nullam cursus pulvinar lectus. Donec et mi. Nam vulputate metus eu enim. Vestibulum pellentesque felis eu massa.

E adesso una nota a piè di pagina.¹ In figura 2 non è riportata alcuna immagine. . . o forse sì?

Scopi della Tesi

Lorem ipsum dolor sit amet, consectetur adipiscing elit. Ut purus elit, vestibulum ut, placerat ac, adipiscing vitae, felis. Curabitur dictum gravida mauris. Nam arcu libero, nonummy eget, consectetur id, vulputate a, magna. Donec vehicula augue eu neque. Pellentesque habitant morbi tristique senectus et netus et malesuada fames ac turpis egestas. Mauris ut leo. Cras viverra metus rhoncus sem. Nulla et lectus vestibulum urna fringilla ultrices. Phasellus eu tellus sit amet tortor gravida placerat. Integer sapien est, iaculis in, pretium quis, viverra ac, nunc. Praesent eget sem vel leo ultrices bibendum. Aenean faucibus. Morbi dolor nulla, malesuada eu, pulvinar at, mollis ac, nulla. Curabitur auctor semper nulla. Donec

¹Nota a piè di pagina.

varius orci eget risus. Duis nibh mi, congue eu, accumsan eleifend, sagittis quis, diam. Duis eget orci sit amet orci dignissim rutrum.

Nam dui ligula, fringilla a, euismod sodales, sollicitudin vel, wisi. Morbi auctor lorem non justo. Nam lacus libero, pretium at, lobortis vitae, ultricies et, tellus. Donec aliquet, tortor sed accumsan bibendum, erat ligula aliquet magna, vitae ornare odio metus a mi. Morbi ac orci et nisl hendrerit mollis. Suspendisse ut massa. Cras nec ante. Pellentesque a nulla. Cum sociis natoque penatibus et magnis dis parturient montes, nascetur ridiculus mus. Aliquam tincidunt urna. Nulla ullamcorper vestibulum turpis. Pellentesque cursus luctus mauris.

Nulla malesuada porttitor diam. Donec felis erat, congue non, volutpat at, tincidunt tristique, libero. Vivamus viverra fermentum felis. Donec nonummy pellentesque ante. Phasellus adipiscing semper elit. Proin fermentum massa ac quam. Sed diam turpis, molestie vitae, placerat a, molestie nec, leo. Maecenas lacinia. Nam ipsum ligula, eleifend at, accumsan nec, suscipit a, ipsum. Morbi blandit ligula feugiat magna. Nunc eleifend consequat lorem. Sed lacinia nulla vitae enim. Pellentesque tincidunt purus vel magna. Integer non enim. Praesent euismod nunc eu purus. Donec bibendum quam in tellus. Nullam cursus pulvinar lectus. Donec et mi. Nam vulputate metus eu enim. Vestibulum pellentesque felis eu massa.

Outline

Il testo della tesi è così strutturato:

Nel primo capitolo è delineato lo stato dell'arte Lorem ipsum dolor sit amet, consectetur adipiscing elit. Ut purus elit, vestibulum ut, placerat ac, adipiscing vitae, felis. Curabitur dictum gravida mauris. Nam arcu libero, nonummy eget, consectetur id, vulputate a, magna. Donec vehicula augue eu neque. Pellentesque habitant morbi tristique senectus et netus et malesuada fames ac turpis egestas. Mauris ut leo. Cras viverra metus rhoncus sem. Nulla et lectus vestibulum urna fringilla ultrices. Phasellus eu tellus sit amet tortor gravida placerat. Integer sapien est, iaculis in, pretium quis, viverra ac, nunc. Praesent eget sem vel leo ultrices bibendum. Aenean faucibus. Morbi dolor nulla, malesuada eu, pulvinar at, mollis ac, nulla. Curabitur auctor semper nulla. Donec varius orci eget risus. Duis nibh mi, congue eu, accumsan eleifend, sagittis quis, diam. Duis eget orci sit amet orci dignissim rutrum.

Il secondo capitolo presenta i risultati della campagna di prove sperimentali Nam dui ligula, fringilla a, euismod sodales, sollicitudin vel, wisi. Morbi auctor lorem non justo. Nam lacus libero, pretium at, lobortis vitae, ultricies et, tellus. Donec aliquet, tortor sed accumsan bibendum, erat ligula aliquet magna, vitae ornare odio metus a mi. Morbi ac orci et nisl hendrerit mollis. Suspendisse ut massa. Cras nec ante. Pellentesque a nulla. Cum sociis natoque penatibus et magnis dis parturient montes, nascetur ridiculus mus. Aliquam tincidunt urna. Nulla ullamcorper vestibulum turpis. Pellentesque cursus luctus mauris.

Nel terzo capitolo si descrivono le scelte di modellazione Nulla malesuada porttitor diam. Donec felis erat, congue non, volutpat at, tincidunt tristique, libero. Vivamus viverra fermentum felis. Donec nonummy pellentesque ante. Phasellus adipiscing semper elit. Proin fermentum massa ac quam. Sed diam turpis, molestie vitae, placerat a, molestie nec, leo. Maecenas lacinia. Nam ipsum ligula, eleifend at, accumsan nec, suscipit a, ipsum. Morbi blandit ligula feugiat magna. Nunc eleifend consequat lorem. Sed lacinia nulla vitae enim. Pellentesque tincidunt purus vel magna. Integer non enim. Praesent euismod nunc eu purus. Donec bibendum quam in tellus. Nullam cursus pulvinar lectus. Donec et mi. Nam vulputate metus eu enim. Vestibulum pellentesque felis eu massa.

Capitolo 1

Focusing for X-rays

“Terence: Rotta a nord con circospezione

Bud: Ehi, gli ordini li do io qui!

Terence: Ok, comante

Bud: Rotta a nord

Terence: Soltanto?

Bud: Con circospezione!”

Chi Trova un Amico Trova un Tesoro

L'introduzione deve essere atomica, quindi non deve contenere nè sottosezioni nè paragrafi nè altro. Il titolo, il sommario e l'introduzione devono sembrare delle scatole cinesi, nel senso che lette in quest'ordine devono progressivamente svelare informazioni sul contenuto per incatenare l'attenzione del lettore e indurlo a leggere l'opera fino in fondo. L'introduzione deve essere tripartita, non graficamente ma logicamente:

1.1 Introduction

Image formation usually implies some form of focusing. How this focusing occurs depends on the way in which the radiation interacts with its surroundings. Thus for visible light the well-known laws of reflection and refraction are utilized, while, while electrons are caused to travel in curved paths in electromagnetic field. X-rays interact with matter in three ways (each causing attenuation of the X-ray beam): elastic scattering, inelastic scattering, and absorption via the photoelectric effect. Elastic scattering (in which exchange of energy is involved) is caused by two process: Thomson scattering from single atomic electrons, and Rayleigh (or coherent) scattering, which occurs from strongly bound electrons acting cooperatively. The scattered and incident beams have a definite phase relationship and interference can occur (Bragg diffraction). Inelastic, incoherent, or Compton scattering occurs from loosely bound (essentially free) electron and involves the transfer of a small fraction of the energy of an incident X-ray photon. The scattered and incident beams do not have fixed relationship, and the atom is raised to a different quantum state due to the excitation of the electron. Absorption (through the photoelectric effect) occurs when the X-ray photon transfer all its energy to an inner atomic

electron, thereby releasing it from atom (ionization)

In Figure 1 the linear attenuation coefficient for these processes are plotted as functions of energy for two materials, carbon and gold, important in soft X-ray physics. For the soft X-ray regime

1.2 Interaction with Matter

When a beam of electromagnetic radiation passes through a material, the intensity is exponentially attenuated

$$I = I_0 \exp(-\alpha x) \quad (1.1)$$

where x is the thickness of the material, α is the linear attenuation coefficient, and I_0 is the intensity at $x = 0$. The amplitude of the electromagnetic wave at x is

$$A = A_0 \exp\left(\frac{-2\pi\beta x}{\lambda}\right) \exp\left(\frac{-2\pi i(nx - ct)}{\lambda}\right) \quad (1.2)$$

where λ is the vacuum wavelength of the radiation, n is the refractive index of the material, and β is its absorption coefficient. The complex refractive index of the material, which governs the propagation of the electromagnetic wave is

$$\bar{n} = n - i\beta \quad (1.3)$$

Since, at soft X-ray wavelengths, absorption is the dominant process, α may be identified with a linear absorption coefficient, where

$$\alpha = \frac{4\pi\beta}{\lambda} \quad (1.4)$$

Tabulation of X-ray absorption data usually give the mass absorption coefficient μ , where

$$\alpha = \mu\rho \quad (1.5)$$

and ρ is the density of the material. The mass absorption of a compound is given by

$$\mu_{\text{com}} = \sum_j w_j \mu_j \quad (1.6)$$

where w_j is the weight fraction of the constituent with mass absorption coefficient μ_j . The linear absorption coefficient of the compound is then

$$\alpha_{\text{com}} = \mu_{\text{com}} \rho_{\text{com}} \quad (1.7)$$

where ρ_{com} is the density of the compound.

In the X-ray region, the energies of individual photons are much larger than the binding energies of outer atomic electron (typically a few electron volts) and molecular binding energies. Absorbing atoms are therefore ionized by the radiation and most of the energy is transferred to the kinetic energy of ejected electron. The energy of an X-ray photon may only be absorbed by an atomic electron from the state. Thus, as the X-ray energy increase, the absorption coefficient will undergo several relatively sharp increases (absorption edges) at energies corresponding to binding energies of different atomic levels. as shown in Figure 1. In practice these increases are not so sharp as indicated, because of the finite energy widths of atomic states and because of the environment of the absorbing atoms.

The theoretical treatment of X-ray scattering and absorption has been given in detail by many authors. A brief summary is included here because the results have implication for the design of X-ray optical system. The starting point of the calculation is to consider the scattering of X rays by free electron (Thomson scattering). An electro-magnetic wave whose electric vector has amplitude A_0 causes such an electron (of charge e and mass m_e) to be accelerated by an amount $A_0(e/m)$. Accelerated charges radiate, the amplitude of the electric vector at a distance r from the charge being

$$A_T(\Phi) = \frac{e}{4\pi\epsilon_0 c^2 r} a \sin \Phi \quad (1.8)$$

where Φ is the angle between the direction \mathbf{r} and the acceleration \mathbf{a} . Thus

$$A_T(\Phi) = A_0 \frac{e^2}{4\pi\epsilon_0 c^2 r} \sin \Phi \quad (1.9)$$

To describe the interaction of an electromagnetic wave with an electron bound in an atom, the Thomson amplitude $A_T(\Phi)$ is multiplied by a complex atomic scattering factor $f_1 + if_2$, so that the scattered amplitude is given by

$$A(\Phi, E) = A_T(\Phi)[f_1(E) + if_2(E)] \quad (1.10)$$

where the factor f_1 and f_2 depend on the energy E of the incoming radiation but it is assumed that, to a first approximation, they do not depend on the scattering angle ϑ (i.e. the angle between the incoming and scattered radiation). This assumption is valid since the wavelengths of interest ($\sim 1 - 10nm$) are larger to typical dimension of the atomic electron distribution ($\sim 1 - 50pm$) so that the atomic electrons may be considered to scatter in phase. The factor f_1 and f_2 can be calculated in relativistic quantum dispersion theory and are given by

$$f_1(E) = Z + 4 \frac{\epsilon_0 m_e c}{h e^2} \int_0^{+\infty} \frac{W^2 \sigma(W)}{E^2 - W^2} dW - \Delta_{(rel)} \quad (1.11)$$

and

$$f_2(E) = 2 \frac{\varepsilon_0 m_e c}{h} E \sigma(E) \quad (1.12)$$

The first term in the equation 1.11 describes Thomson scattering (Z is the atomic number of scatterer) and, to describe the angular dependence of the scattering, may be replaced by the angle-dependent form factor

$$f_0 = \int_0^{+\infty} U(r) \text{sinc}\left[\frac{4\pi r}{\lambda} \sin \frac{\vartheta}{2}\right] dr \quad (1.13)$$

where $U(r)$ is the radial charge distribution and $\text{sinc}(x) = \frac{\sin x}{x}$. If the wavelength λ is in nanometres, then for $\sin \frac{\vartheta}{2} \leq \frac{\lambda}{2}$, $f_0 = Z$, while for $\sin \frac{\vartheta}{2} = \lambda$, $f_0 \simeq 0.9Z$ for most elements.

The second term in 1.11, the anomalous dispersion integral, is the same as that given semiclassically by considering the electrons to be caused to oscillate by the incoming radiation. Because it neglects damping, this term results in imprecise values for f_1 close to absorption edges. The atomic photo ionization cross section $\sigma(E)$ (in $m^2 \text{atom}^{-1}$) is related to the mass absorption coefficient by

$$\sigma(E) = A \frac{\mu}{N_0} \quad (1.14)$$

where A is the atomic weight and N_0 is Avogadro's number. In order to calculate $\sigma(E)$ theoretically the atomic wave function must be known; these have to be obtained by approximation methods for all systems except hydrogen, leading to uncertainties in the expressions for f_1 and f_2 .

The third term in equation 1.11 is a relativistic correction, which is negligible at X-ray energies (except near absorption edges) to assume that the solid state environment does not greatly affect the ionization process, since it is the outer atomic levels that are most modified when an atom is bound in a solid. Then, the atomic parameters f_1 and f_2 may be related to macroscopic factors n and β by

$$\delta = 1 - n = \frac{e^2 \hbar^2}{2\varepsilon_0 m_e E^2} \overline{f_1} \quad (1.15)$$

and

$$\beta = \frac{e^2 \hbar^2}{2\varepsilon_0 m_e E^2} \overline{f_2} \quad (1.16)$$

where f_1 and f_2 are the average atomic scattering factors per unit volume,

$$\overline{f_1} = \sum j N_j f_{1j} \quad \overline{f_2} = \sum j N_j f_{2j} \quad (1.17)$$

and N_j is the number of atoms of type j per unit volume. For energies well away from any absorption edges, equation 1.15 reduces to

$$\delta = \frac{Ne^2\hbar^2}{2\varepsilon_0 E^2} = \frac{Ne^2\lambda^2}{8\pi^2\varepsilon_0 m_e c^2} \quad (1.18)$$

where N is the total number of electrons per unit volume. This equation 1.18, is the same as that originally derived by Lorentz using classical ideas of absorption. In X-ray region, δ is small (typically $\sim 10^{-3}$) and positive, i.e., the refractive index for soft X rays is slightly less than unity. Tables of values for f_1 and f_2 have been published, and these were used to generate Figure 1, along with the experimentally observed variation of the absorption coefficient away from an absorption edge:

$$\beta \sim Z^2 \lambda^3 \quad (1.19)$$

1.3 Total External Reflection

The propagation of X rays in matter may be described by the complex refractive index

$$\overline{n} = n - i\beta = 1 - \delta - i\beta \quad (1.20)$$

where δ is small and positive. Thus the real part of the refractive index is, unlike the case for visible light, less than one and so, if a normal refractive lens were to be used for focusing, it would have to be concave to give a real focus for an incident plane wave. For a plano-concave lens with central thickness d (Figure 1.19)

$$\frac{f}{\rho} = 1 + \frac{n}{\cos \varphi - n \cos \varphi'} \quad (1.21)$$

where f is the focal length, ρ is the radius of curvature of the concave surface, and φ and φ' are the angles with respect to the normal to the concave surface as defined in Figure 2. For axial rays, this becomes

$$\frac{f}{\rho} = 1 + \frac{n}{1 - n} = \frac{1}{\delta} \quad (1.22)$$

The depth of focus of such a lens is given by

$$\Delta f = \pm \frac{1}{2} \left(\frac{f}{r} \right)^2 \lambda \quad (1.23)$$

where r is the radius of the lens aperture and λ is the illuminating wavelength. The maximum thickness of lens is, from Figure 2 ,

$$t = \rho - (\rho^2 - r^2)^{\frac{1}{2}} + d \quad (1.24)$$

The closeness of the refractive index to unity, and the high absorption of soft X rays, means that lenses of the same sort of dimensions as those used for visible light would have impossibly long focal length ($\geq 10m$), very small depths of focus (\sim tens of micrometers), and they would absorb essentially all of the incident radiation. Thus this type of lens is impractical for X ray, as has been stated by previous authors.

However, optical components currently in use for X rays can have focusing effective of about 10% and effective aperture radii of about $10 - 50\mu m$. To match this efficiency, a refractive lens should have a mean thickness such that about 10% of the incident intensity is transmitted. Two possible lenses, for soft-X ray wavelength of about $3.5nm$, are shown in Table 1. These results show that such lenses may not be unreasonable, although they have very large f-number and so very intense source would be needed to prevent long imaging times. Calculation for biconcave lenses give similar results. However, the exact focusing property of soft X-ray refractive lenses depend on a better knowledge than currently available for the optical constants, and to date no attempts have been made to manufacture them.

The other conventional method of focusing at visible wavelengths is to use refractive optics. The reflected amplitude, a , at an interface between vacuum and a material is given by the Fresnel equation. For radiation polarized so that the electric vector is perpendicular to the plane of incidence (s polarization)

$$a_{\perp} = \frac{\cos \varphi - (\bar{n}^2 - \sin^2 \varphi)^{\frac{1}{2}}}{\cos \varphi + (\bar{n}^2 - \sin^2 \varphi)^{\frac{1}{2}}} \quad (1.25)$$

where the angle of incidence φ is measured from the surface normal. In terms of the glancing angle, $\vartheta = 90^\circ - \varphi$, this becomes

$$a_{\perp} = \frac{\sin \vartheta - (\bar{n}^2 - \cos^2 \vartheta)^{\frac{1}{2}}}{\sin \vartheta + (\bar{n}^2 - \cos^2 \vartheta)^{\frac{1}{2}}} \quad (1.26)$$

For parallel polarized radiation (p polarization)

$$a_{\parallel} = \frac{\bar{n}^2 \sin \vartheta - (\bar{n}^2 - \cos^2 \vartheta)^{\frac{1}{2}}}{\bar{n}^2 \sin \vartheta + (\bar{n}^2 - \cos^2 \vartheta)^{\frac{1}{2}}} \quad (1.27)$$

The reflectivity is given by

$$R = \frac{I}{I_0} = aa^* \quad (1.28)$$

where I_0 is the incident intensity and I is the reflected intensity. For radiation incident normally on a surface, $\vartheta = 90^\circ$ and equations 1.26 and 1.27 both lead to the normal incident reflectivity

$$R_n = \left(\frac{1 - \bar{n}}{1 + \bar{n}} \right)^2 = \frac{\delta^2 + \beta^2}{(2 - \delta)^2 + \beta^2} \quad (1.29)$$

Using the values given in Table 1, and equation 1.4, gives, for a wavelength of $3.5nm$, $R_n = 3.3 \times 10^{-6}$ for carbon and $R_n = 4.6 \times 10^{-5}$ for gold. Normal incidence reflectivity are very small for all material over soft X ray range, which means that conventional mirror used in this way are impracticable.

1.4 Enhancement of Reflectivity

The reflectivities of surfaces for X rays wavelength may be increased by using grazing angle incidence. If, in equation 1.26 and 1.27, the glancing angle is such that

$$(\bar{n}^2 - \cos^2 \vartheta)^{\frac{1}{2}} = 0 \quad (1.30)$$

then the reflectivity is identically equal to unity. For a non absorbing medium ($\beta = 0$), total reflection is obtained for glancing angles smaller than the critical angle ϑ_c , where

$$\cos \vartheta_c = n = 1 - \delta \quad (1.31)$$

For real media, the reflectivity approaches unity as $\vartheta \rightarrow 0$. If $\beta \ll \delta$ a sharp increase in reflectivity is obtained as ϑ fall below ϑ_c ; for $\beta \sim \delta$, a more graduate transition occurs. For $\vartheta < \vartheta_c$ no wave can propagate in the mirror material and the incident energy is reflected ("total external reflection"). Calculated grazing incidence reflectivity (for s polarization) are shown for beryllium, carbon, and gold at $\lambda = 3.5nm$ in Figure 1. The p-polarization reflectivity not significantly different. A major problem with grazing incidence optics is their severe aberration, especially astigmatism that can be .

Capitolo 2

Mirrors for X-rays

“Terence: Tu lo reggi il whisky?”

Bud: Beh, i primi due galloni si, al terzo divento nostalgico e ci può scappare la lite... E tu lo reggi?”

Terence: Eh, che domande, io sono stato allattato a whisky!”

I due superpiedi quasi piatti

A spherical surface is defined by only one parameter, the radius of curvature of the surface. A spherical surface has the property that the rate of change of the surface slope is exactly the same everywhere on the surface, and thus the aberration is inevitable. This shape bring an intrinsic aberration ("spherical aberration"). If a beam having rays parallel to the optical axis, with a big aperture, hits a concave mirror, as shown in Figure 3, the rays will not focus in the same point "focus", but they converge at the circumference of a circle. So, the image, is not any more a single point but a spot, beams at different position have different focal points. Consider ray AB parallel to the optical axis at a distance d from it. After the reflection of the mirror AB intercept the optical axis at the point F' from the origin O. The relation between F' , the radius of the mirror R and the distance d is

$$\frac{f'}{R} = 1 - \frac{1}{2\sqrt{1 - \left(\frac{d}{R}\right)^2}} \quad (2.1)$$

Equation ?? can be obtained by Figure 4. BF' is the reflected ray of the non-paraxial ray AB, F' is the intersection point with the optical axis. Because the law of reflection

$$\alpha = \beta \Rightarrow \alpha = \gamma \quad (2.2)$$

Therefore $F'BC$ is isosceles and $F'D$ is both median and height, thus

$$DC = \frac{R}{2} \quad (2.3)$$

From the right-angle triangle $F'DC$ we obtain

$$\cos \gamma = \frac{R}{2F'C} \Rightarrow F'C = \frac{R}{2 \cos \alpha} = \frac{R}{2\sqrt{1 - \sin^2 \alpha}} \quad (2.4)$$

From the right-angle triangle CGB

$$\sin \alpha = \frac{d}{R} \quad (2.5)$$

The last two equation combined with

$$OF' = OC - F'C \Rightarrow f' = R - F' \quad (2.6)$$

When $\frac{d}{R} \rightarrow 0$ then $\frac{f'}{R} = \frac{1}{2}$, therefore

$$f' = \frac{R}{2} \quad (2.7)$$

and the mirror is ideal

If the slope is not any more constant all over the mirror but become flatten in the region surrounding the outer rays, it is possible to focus all the rays in the same point. While correction of spherical aberration is not the only application of aspherical surfaces, it is one of the major application areas. On the contrary from spherical surface, aspherical surfaces cannot be defined with only one curvature, this kind of aspherical surfaces are usually defined by an analytical formula. There exist different kind of aspherical surface with different properties, if there is not the rotational symmetry it is possible to have either a *biconic* surface with two basic curvature and two conic constant in two orthogonal direction or as an *anamorphic sphere*, which has additional higher-order terms in two orthogonal directions. Another form of aspheric surface is a *toroidal* or *toric*. This shape is a surface of revolution with a hole in the middle, like a doughnut, forming a solid body. This shape is characterized by two radii, the overall outer radius and the smaller cross-sectional radius. The good point of this geometry is the minimization of astigmatism that make it possible to focus on a small spot, differently from the spherical ones.

2.1 Conic Surfaces

A special kind of aspherical surfaces is those named "*conic surfaces*" that can be defined as

$$z = \frac{cr^2}{1 + \sqrt{1 - (1 + k)c^2r^2}} \quad (2.8)$$

where c is the base curvature at the vertex, k is a conic constant, and r is the radial coordinate of the point on the surface. In Table 2.1 it is shown how the different shape are obtained changing the conic constant k

A good point that have the conical surfaces are the no-presence of spherical aberration. If the object is at the center of curvature of the surface there are no aberration. Considering an ellipsoid, it is possible to form aberration-free-image for a pair of real image, similar to a hyperboloid mirror. For parabolic mirror there is only one point

Conic Constant k	Surface Type
0	Sphere
$k < -1$	Hyperboloid
$k = -1$	Paraboloid
$-1 < k < 0$	Ellipsoid
$k > 0$	Oblate Ellipsoid

Tabella 2.1: Parameter of different conic surfaces

that make a perfect image of a point for an axial object at infinity. This parabolic behaviour is the main point that make those mirror widely used in astronomical optics. Moving axially the object from the free-aberration point induce a certain amount of spherical aberration: If the movement is laterally, different type of aberration are induced such as: coma, astigmatism.

2.2 Compound Optical system

A further step to obtain a better image is that to use a more than one mirror in order to have a perfect image at the focus. The system that were invented which respect the sine-Abbe-condition are the Wolter system that are widely used in astronomy, using combinations of coaxial and confocal conic section. A first approximation system that respect the sine Abbe condition are the Kirkpatrick-Baez system and Montel or nested-Kirkpatrick-Baez system, those compound optical system involves reflector whose meridian planes are at right angle (crossed).

2.2.1 Sine Abbe condition

2.2.2 Wolter System

In 1952 Wolter published a paper in which he discussed several disposition of two conical mirror in order to collect light for an astronomical use. Figure show the different disposition discussed: Wolter I, Wolter II, Wolter III. Wolter I telescope consist of a coaxialparaboloid (primary mirror) and hyperboloid (secondary mirror). The focus of the paraboloid is coincident with the rear focus of the hyperboloid, and the reflection inside both mirrors. The Wolter II telescope use the same kind of mirror of Wolter I paraboloid and hyperboloid. But the focus of the paraboloid coincident with the front focus of the hyperboloid, and, the reflection, occurs internally for the paraboloid and externally for the hyperboloid. The Wolter III telescope consist in a paraboloid and an ellipse. In this system the first mirror is the paraboloid one, and the second is the ellipsoidal that have front focus coincident with that of the parabola, moreover the reflection is external for the paraboloid and internal for the ellipsoidal. The Wolter I have typical grazing angle of less than a degree and is used for hard X-rays. The Wolter II telescope has typical grazing angle of, approximate, 10 degree and is used for soft X rays and extreme ultraviolet (EUV). Because of circular symmetry, astigmatism and spherical aberration are eliminated

but exhibit coma aberration. Other problem is the difficulty of fabrication , and require a huge area to achieve a very small collecting angle.

2.2.3 Kirkpatrick-Baez System

This kind of optics are used in the ESRF and consist, as shown in Figure, in two separated cylindrical surface conical mirror that focus the incident beam in both sagittal and transverse thus astigmatism is removed. Although such system introduce another type of distortion, anamorphotism. Because of the different distance of the image plane with respect to the mirrors the magnification is different in the two direction. Another technical problem that face with system is the big volume that occurs to implement it. To overcome those two problem and obtain a system that conjugate the good behaviour of the KB system with an equal magnification of the two direction and compact system, it is possible to implement a system as it is showed in Figure, a system in which both mirrors are at the same distance from the object. This sort of arrangement is extremely difficult to manufacture and, consequently, very expensive. Despite these problem K-B system are very used in ESRF and in European synchrotron, on the contrary, in American synchrotron another type of optical system, named "Montel", is used that will be discussed in the next section.

Capitolo 3

Montel System

As discussed before KB system have some limitation that can be overcome with a different optical system named "Montel". This geometry brings four important advantages for high-precision focusing:

- i) the optical system is more compact which allows greater working space;
- ii) the focal distance of the two mirrors are the same, this cancels out the anamorphism;
- iii) the alignment of the system is easier with respect to the KB system because, in this case, only one thing has to be aligned, on the contrary, in the KB there are two separated mirrors that have to be aligned;
- iv) the divergence that can be collected is larger which allows for greater flux and/or a lower diffraction limit.

3.0.1 Optical Design

The mirrors used in this Montel configuration are mirrors that have a cylindrical shape in one direction and elliptical shape in the other direction. One approach to obtain the Montel system is that to use two pre-figured elliptical mirrors and grind the cut site at 45° as shown in figure. After that it places the mirrors together makes a good fit with no gap requiring no contouring of the mirror side. Another way involves dividing pre-figured elliptical mirrors into two parts that, added together, can form the Montel system. This approach is primarily driven by the fact that in a conventionally polished mirror, the clear aperture area has the best figure and finish. As such uAs such, using two halves of a prefigured mirror cut in the middle has several advantages- including consistency and economy. There are major challenges however. First, the mirror surface must be protected against damage and deformation during cutting and subsequent figuring operations. After cutting into two, the cut sites must be treated (e.g., etched) to remove any subsurface damages that could alter a mirror's figure. Then the mating side of one of the mirrors must be contoured and polished such that when it is placed against the partner mirror, it makes a nearly perfect fit with good surface quality all the way to the contact edge. These last two steps are crucial because if there is a significant gap or if the mirror surfaces in the vicinity of the interface are damaged, a significant part of the incident beam could be lost. As an example, we are developing a pair of Montel

mirrors for polychromatic nanofocusing on Sector 33 at APS. This beam line will use 40 mm long elliptical mirrors for nano-focusing a 100 μm beam to a 50 nm spot at 2000x demagnification. This concave elliptical mirror has a maximum depression of about 6 μm at its center. If cut flat and placed against its mating mirror, a gap as large as 6 μm is created which loses about 10% of the 100 μm incident beam. Similarly, if the mirror surfaces near the intersection are damaged, then beam loss can be significant.

Capitolo 4

Mt script

“Bud: No, calma, calma, stiamo calmi, noi siamo su un’isola deserta, e per il momento non t’ammazzo perché mi potresti servire come cibo ...”

Chi trova un amico trova un tesoro

My thesis’ work is the creation of a python script that simulate a ray-tracing of a beam. This tracing take in account the effect of different type of optical elements that that can find the beam in its way. To implement this ray-tracing it have to define three elements:

- source
- optical elements
- tracing system

4.1 Source

The beam source is characterized by two parameters: spot dimension divergence. For the geometry dimension is possible to choose between a spot of uniform ray in a rectangular or circular shape or a gaussian profile with a parameters setted by the users (radius for the circular case, two sides for rectangular shape and FWHM for Gaussian profile), there is the possibility to choose a point-wise shape for the source. Also the divergence profile have different possibilities, there is the Gaussian profile, with FWHM as parameter, rectangular flat divergence, with two side as parameters, and a collimate one. for the setting parameter of the source shape there are no limitation, but for the divergence parameters, because of the normalization of the velocity, be careful on the parameter’s values. Figure 1 shows an example of circular shape for the source beam, and Figure 2 shows a gaussian profile. It is choose a red marker for the plot of the real space, and blue marker for the plot of the divergence.

4.2 Optical Elements

There are implemented two kind of optical elements in the script: lens and mirror. Because, as discussed in Chapter 1, mirrors are the principal elements used

in synchrotron, more attention is focused on them, on the contrary, for testing uses, only one kind of lens, an ideal lens, is implemented.

4.2.1 Mirrors

It is possible to choose a mirror that have shape of: plane, sphere, ellipse, parabola and hyperbola. All this mirror to have a conical shape in two dimension, or a conical shape in one dimension and cylindrical in the other, moreover is possible to set a dimension of the mirrors that, in the default case, are setted as infinite mirrors. The mirrors are expressed in a Cartesian defined as surface conical equation with a characteristic focal parameter depending on their nature, for plane mirror no parameter are needed, for spherical mirror only one focal distance is needed, for parabolic mirror is needed one focal distance plus a term that define the nature of the mirror and, for ellipsoidal and hyperbolic mirror, two focal distance are needed, moreover, apart for the plane mirror, also the incidence angle is needed to determine the shape of the mirror. The surface conical equation is determined such that the origin of the cartesian system correspond to the point where the optical axis hit the mirror and the normal correspond to the z-axis. To understand better the situation look at Figure 2, that report an ellipsoidal mirror characterised by two focal distance equal to p and q , and an angle of incidence equal to ϑ , and also, it is possible to see the dimension of the mirror.

FIGURE

In the appendix A is reported the calculation of the changing from system solidal with the mirrors.

4.2.2 Lens

As said before the only lens defined is an ideal lens that bring the entrance beam and, following the typical equation 4.1 of a lens, do the correct transformation

$$\frac{1}{f} = \frac{1}{p} + \frac{1}{q} \quad (4.1)$$

As reported in equation 4.1, the parameter needed to characterize the lens is f , in the 3D system, a lens is defined by two parameter f_x and f_z , that define the focal distance for the two direction and, those parameter, are the parameter that the users have to define in order to use the ideal lens in the program.

4.3 Tracing System

Defined the source and the different optical element, to have a simulation, is needed a tool that put everything together and modify the property of the beam after the interaction with the optical elements.

Before to trace the system is important to define the system, in other word is important to locate the position of the optical elements. The program is written in such a way that the tracing system work in series one optical element after the other, and, for every element, it have to define the object plane distance and the

image plane distance, that can be different from the focal distance which are defined as default. For example, if we want to simulate a system such that reported in figure 3, we have to define firstly the mirror and after there are different possibilities to define the tracing distance, one possibilities is that.

Figure Going deeper in the code, the algorithm that trace a single element is divided in 5 step

1. change the reference system with that soldal with the optical element after two rotation, one along x-axis, and second along y-axis, and a translation equal to the object distance of the optical element
2. free propagation up to the optical element
3. effect of the optical element
4. free propagation to the image plane
5. changing the Cartesian system in that one that have the optical axis equal to the y-axis

FIGURE

4.4 Compound Optical Element

This program include also two different system composed by more mirrors. Starting from more surface conical mirror, combining them, is possible to have a compound optical elements that can simulate the behaviour of some typical instrumentation that characterize the facilities, in particular the synchrotron environment. The compound optical include are two of those mentioned in Chapter 2

- KirkPatrickBaez system (KB system)
- Montel

4.4.1 KirkPatrickBaez System

KirkPatrickBaez or, more simply, KB system are shown in Figure 2 are two cylindrical surfacing conic mirror placed one after the other with the two focal lens that converge in the same point. There are implemented two different kind of KB system, a one composed by elliptical mirrors and a second one composed by parabolic mirrors. The parameter parameter that needed to the program that define the system are two focal distances and the two incidence angle that define the two surface conic, in the default mode the two angle are identical.

FIGURE

Because this system is simply a system composed by two surface conical mirror in series the parameter that the system need to define the mirror are no the ones defined by the user but are the focal distance of the two mirrors that are, as shown in Figure, p_1 , q_1 , p_2 , q_2 . The parameter p and q are, respectively, the distance

of the first focal point to the center of the system, and the distance between the center of the system to the second focal point. This system can do two different thing, the first one is to focalize a beam in a point, the second one is to collimate a beam, obviously this work if the system is defined with the correct parameters.

4.4.2 Montel System

FIGURE

This compound optical system is defined, as defined for KB, from the definition of two cylindrical conical surface rotating, one of them, of 90° , in order to have a mirror in the xy plane, and another one in the zy plane. As shown in Figure 2 the center of the Cartesian system is setted in the point where the optical axis of the system hit the compound system having the normal of the first normal equal to the z-axis, and the second normal equal to the -x-axis. The system is defined by the following parameter p , q , ϑ_z , ϑ_x , where p and q are the focal distance of the two mirrors and ϑ_z and ϑ_x are the angle of incidence to define the correct mirrors (by default $\vartheta_z = \vartheta_x$).

Another parameter that can be setted to this system is the value of the angle that there is between the first optical element and the second one. As for the KB system also in this case there are the two cases, an ellipsoidal system (having the two mirror as ellipsoid), and parabolic system (having the two mirror as ellipsoid). The aim of the Montel, as for the KB, is that to work on the two dimension of the beam for each mirror, such that to localize the system on the same point, or collimate the beam in the two direction.

4.5 Tracing system for compound optical elements

Because of the different definition, the tracing method of the rays' beam, need a different interpreter that can link the beam with the different optical elements that meet on his way. Because of the different nature, there are implemented two kind of tracing, a first one that trace the KB system, that is composed by a series of optical elements and so can be used for all the compound optical elements that are in series. And a second one that is specific for the Montel system, because it is not composed by mirrors in series rather than mirrors in parallel, having the two elements in a very small region of the space that have in which order the rays of the beam hit the different mirrors.

4.5.1 Tracing for KB

For KB system the situation is more or less the same as for a simple optical mirrors, with the only difference that there are more than one mirror. So the algorithm to simulate the tracing system is nothing else than a for loop, that use the tracing system of the simple optical element. In this case is needed the object and the image distance from the center of the system, as for the optical element tracing, that are set by default as the focal distances, and the incidence angle of

the two mirror, that, by default, are the ones in which the mirrors are designed. As shown in Figure, having the object and image distances, and using the trace elements defined for one mirror, there is one degree of freedom, that is the Figure (sistemare bene questa parte qui)

4.5.2 Tracing for Montel

Montel system is completely different from the KB system and all the series optical system, so it need a new trace system. This new trace system is divided as follow

1. Changing the reference frame in one having the center on the center of the mirrors, with a z-axis corresponding to the normal of one mirror and -x-axis equal to the normal of the second mirror. This transformation is done in a similar way of the normal tracing, two rotation of the beam, and one translation, differently from the normal tracing, the tw rotation are done such that the beam hit the mirrors with an incidence angle set by the user
2. Focus the attention on the travel time of each ray in order to know which is the nearest optical element of each ray
3. free propagation of each ray up to the nearest optical element
4. effect of the system for each ray
5. repeat the 2nd, 3rd and 4th passage two times, in order to consider the two reflection
6. Change the reference system solidale with the beam that is subject to two reflection, doing two rotation and one translation

What is reported above is the default tracing system that, because of its centrality on my thesis' work have many option. What is setted by the user is

1. focal distances and incidence angles, that define the two rotation and the translation of the tracing system
2. name of the File in which is saved the data of the simulation, by default no data is saved
3. there is the possibility to choose a different point, from the origin, in which the the optical axis hit the system
4. there is also the possibility to have a final output frame that is not solidal by the two-reflected beam, but with the non reflected beam or with the other two beam that are reflected only one time
5. It is also the possibility to figure out the footprint of the two reflected beam on the system. For clarity the beam that hit the first mirror and after the second is labelled with red point, the beam that hit the second and after first mirror is labelled by blue color

These options are added in order to study better the behaviour of a beam with a Montel system. The possibilities to change the angle of incidence and to hit different part from the origin can be used to study what happen to a beam when is not aligned, or not perfectly aligned, and use these result to align the system in the laboratories. The possibilities to save a File is useful in particular in those case where there is a huge computational effort that need a lot of time, in these cases is possible to work with the result of a big simulation without reappointing it, and so save time.

Capitolo 5

Results

*“Terence: Ma scusa di che ti preoccupi, i piedipiatti hanno altro a cui pensare, in questo momento stanno cercando due cadaveri scomparsi
Bud: Se non spegni quella sirena uno di quei due cadaveri scomparsi lo trovano di sicuro!”*

Nati con la camicia

A comparison of the simulation with respect to the software OASYS developed by Manuel Sanchez Del Rio and with a paper [RKM15] in order to demonstrate the correct operation of the program. The comparison with OASYS check the work of all the component apart from Montel system (mirrors, lens, KB ...), the paper is dedicate for the Montel system, because this particular kind of optical system is not implemented on OASYS.

5.1 Testing with OASYS

5.2 Testing with the paper

The system simulated in the paper have the following parameter: a source with a Gaussian shape with a FWHM of $2.5\mu\text{m}$ and a Gaussian divergence of 5mrad . Moreover, as shown in Figure 5.1, the position of the Montel system from the source is $\simeq 0.26\text{m}$ and the image plane is located at 10.06m from the center of the Montel system, with an incidence angle $\vartheta \simeq 2.86^\circ$.

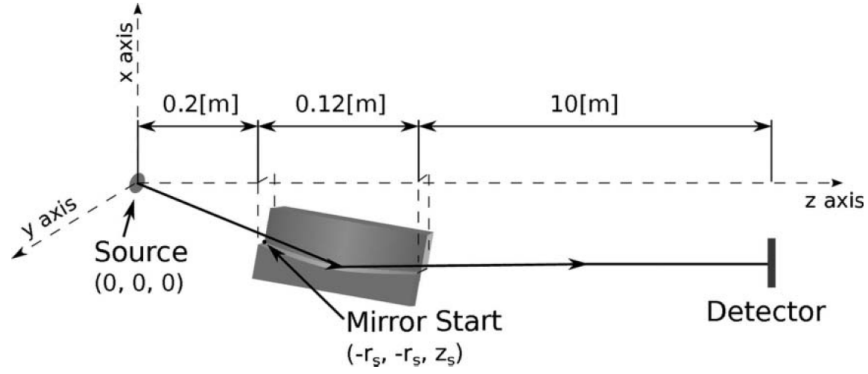


Figura 5.1: Illustration of the Montel system used as a collimator in the paper [RKM15]

The result of the geometry and the divergence of the beam at the image plane, after the double-reflection of the Montel system, is showed in Figure 5.2. Where, in Figure 5.2a, is showed the real image of the beam at the image plane, and, in Figure 5.2b, is showed the divergence. The quantitative values reported on the paper says that the profile of the beam correspond to a Gaussian-like distribution with a spacial FWHM of $\sim 0.7\text{mm}$ and a FWHM's divergence of $\sim 0.01\text{ mrad}$. The results of the system defined in the paper [RKM15], are figured out in Figure 5.3. As is shown in the Figure 5.3 there is a qualitative good agreement with the two simulation, .Also, under a quantitative point of view, there is a good agreement in fact, in simulation are obtained a value of $\sim 1\text{mm}$ of FWHM of image size, pretty similar to the one of the other simulation, and $\sim 0.01\text{ mrad}$ FWHM of divergence that is equal to the one obtained with the other simulation.

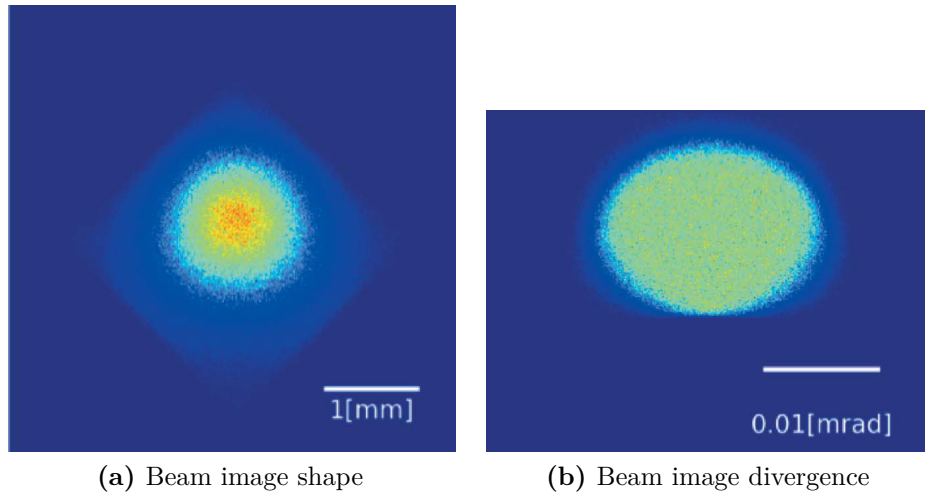


Figura 5.2: Results of the Montel system of a source beam with a FWHM spot of $2.5\mu\text{m}$ and a Gaussian divergence of 5mrad

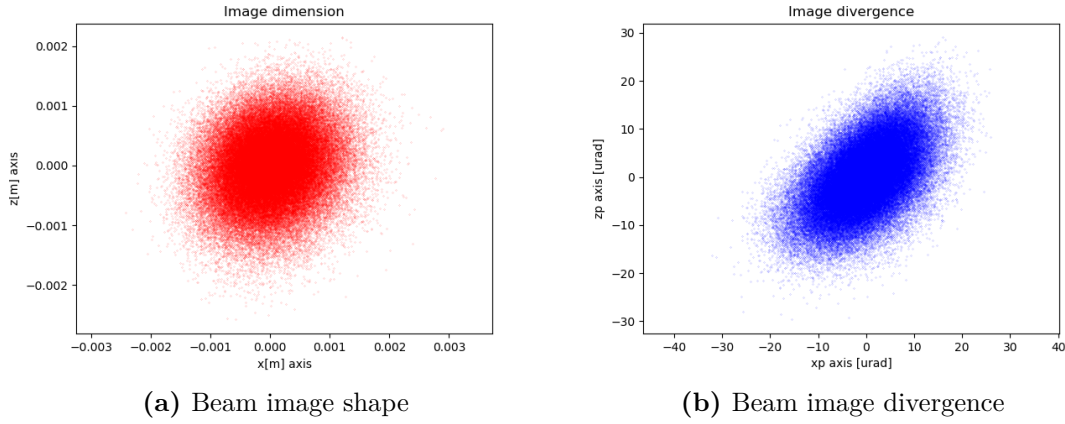


Figure 5.3: Results of my Montel simulation of a source beam with a FWHM spot of $2.5\mu\text{m}$ and a Gaussian divergence of 5mrad

5.3 Analysis of Montel system

To understand the Montel system is used the program defined, simulating different situation, studying the results obtained. To understand that Montel work well, it is simulated the behaviour of a pointwise source with a certain divergence, using a collimating system, and watching what happen to the beam. The second step is to simulate a collimating beam with a certain source shape geometry and figure out the image plot obtained by a focalizing system in its image plane. What is expected is a point, in the velocity space for the first situation and in the real space for the second simulation, because this is the behaviour of an ideal collimating/focalizing system. For the simulation are used parabolical Montel and an incidence angle of 2° (the choice of the angle is arbitrary, that of the paraboic system is because is needed to collimate a beam, also for elliptical system is possible to tcollimate a beam using one focal distance very big). For the collimating system

5.4 Alignment

Alignment of a beam is important for experimental use so, this section studies the behaviour of a beam when the beam is not perfectly align, in order to understand the behaviour of the beam in the different cases and act consequently. The parameter that are changed are :

1. orthogonality
2. incidence angle
3. point of incidence

Using a focusing parabolic Montel system with a source of square shape having a side of $1\mu\text{m}$, and a Gaussian divergence with FWHM of $25\mu\text{m}$

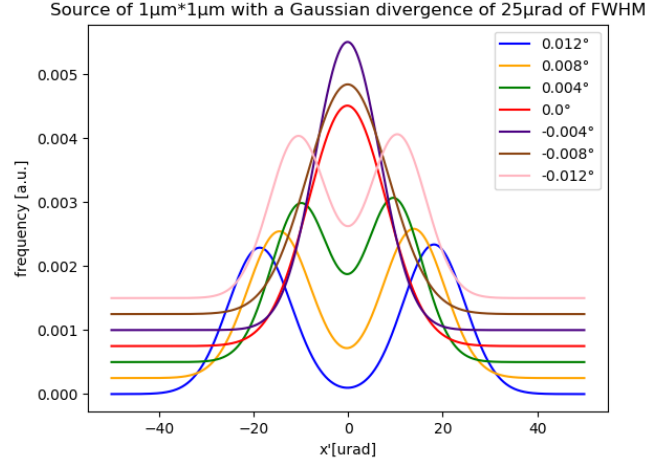


Figura 5.4: Nessuna immagine... Sorry.

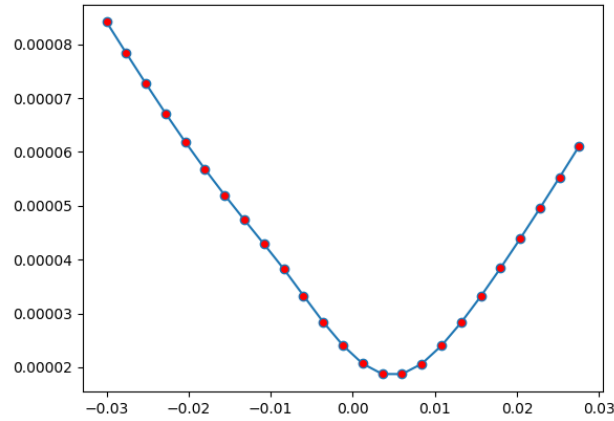


Figura 5.5: Nessuna immagine... Sorry.

5.4.1 Orthogonality

In this section is it done an orthogonality studies of the Montel system, it is studied the behaviour of a beam, using a source parameter defined before. Figure 5.4 presents the interesting histogram versus the horizontal angle x' when the angle between the mirrors change ($\alpha = 90^\circ + \Delta$). It can be noted a improvement of the collimation of the beam changing the angle in the case of closer mirrors ($\Delta = -0.004^\circ$).

Figure show the trend of the FWHM of the x' changing the angle Δ , it is possible to note a minimum for negative angle (this situation correspond to the indigo line) after that the situation become worse. Moreover, the behaviour of the FWHM is not symmetric with respect to 0° , in case of negative angle deviation the situation improve for small range of deviation angle, after that, the trend get worse, on the opposite way, the situation get worse increasing the positive deviation angle.

5.4.2 Incidence angle

5.4.3 point of incidence

Another way that can be studied to align correctly a beam, is to study the behaviour of a non centred beam with respect to the center of the Montel system. In this section is reported the behaviour about the change of FWHM of both x' and z' following different path. Figure 5.6 show the different path followed to simulate the non-centred beam that are named:

1. Y
2. XZ
3. XYZ1
4. XZY2

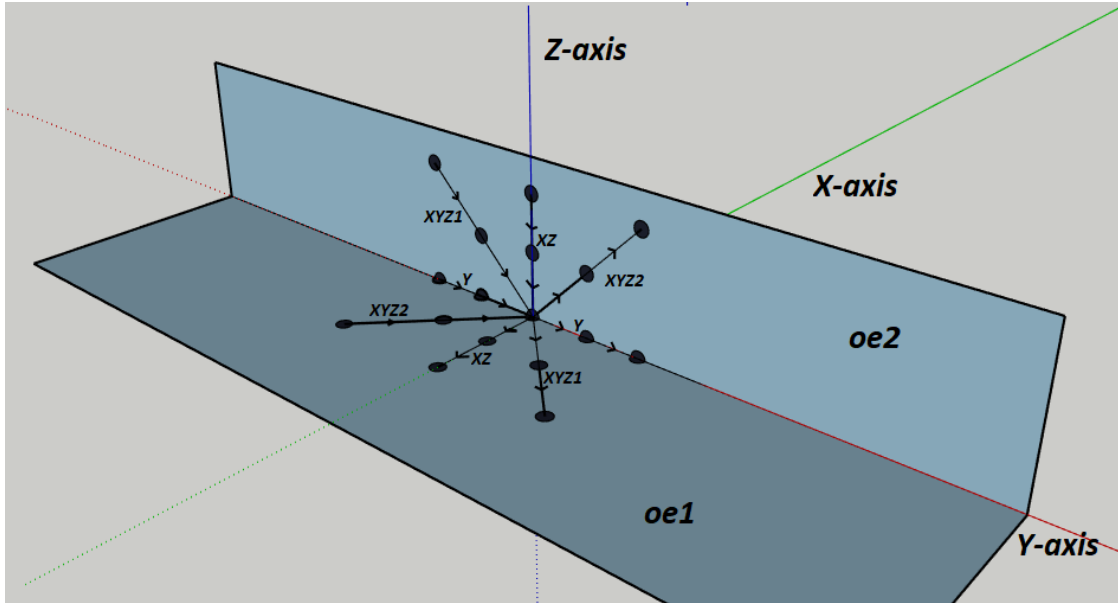
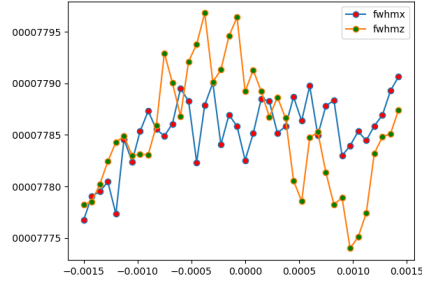


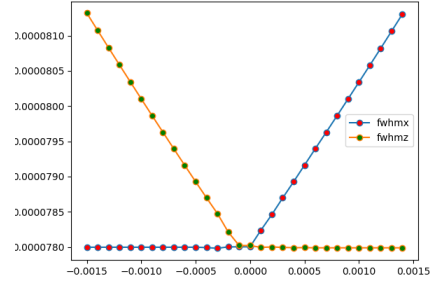
Figure 5.6: Different path for simulate the non-centred beam

Figure 5.7 show the behaviour of the two FWHM of the beam changing the incidence point of the beam moving the different paths. This point is defined with respect to the center of the Montel system that correspond to the origin $(0, 0, 0)$. In Figure 5.7a, the incidence point move along y-axis, start from the point $(0, 1.5\text{mm}, 0)$ and arriving to the point $(0, -1.5\text{mm}, 0)$, and show, more or less, a flat behaviour of the FWHM. Figure 5.7b start from the point $(0, 0, 0.15\text{mm})$ and arrive to $(-0.15\text{mm}, 0, 0)$ and have specular behaviour for the two FWHM, there is a minimum of the two FWHM near the origin point, moving on the oe1 worse the FWHM of z' and maintain the other constant, on the contrary, moving on the oe2 the situation is reversed, in this case the FWHM of x' get worse, maintaining constant the one of z' . Figure 5.7c start from $(0, 1.5\text{mm}, 0.15\text{mm})$ and arrive to $(-0.15\text{mm}, -1.5\text{mm}, 0)$ and Figure 5.7d start from $(-0.15\text{mm}, 1.5\text{mm}, 0)$ and arrive

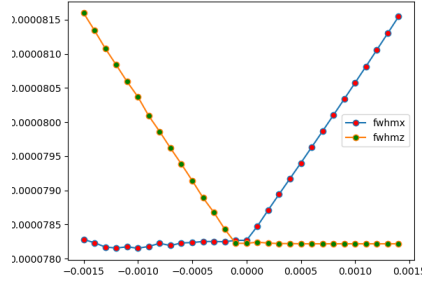
to $(0., -1.5\text{mm}, 0.15\text{mm})$. The behaviour of this last two path are similar to that of 5.7b, this is reasonable, because the motion along y-axis does not influence the FWHM because of the definition of the cylindrical mirror, that in any point along the y direction have the same geometry.



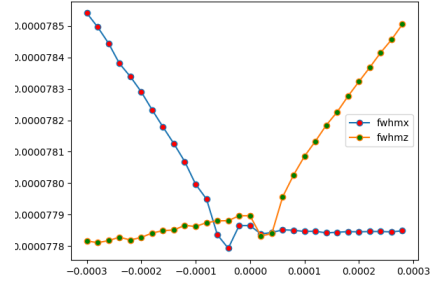
(a) Y path



(b) XZ path



(c) XYZ1 path



(d) XYZ2 path

Figure 5.7: Results of the Montel system of a source beam with a FWHM spot of $2.5\mu\text{m}$ and a Gaussian divergence of 5mrad

Capitolo 6

Prove Sperimentali

6.1 Sezione

La figura 6.1 [nella pagina successiva](#) riporta alcuni grafici di esempio, creati con MatLab ed esportati in formato vettoriale (.eps), con griglia in ogni grafico, box esterno, e dimensione del font adeguata per la tesi stampata. In tabella 6.1 sono invece riportate le principali caratteristiche (inventate) della camera di prova di una galleria del vento.

6.1.1 Subsection

Lorem ipsum dolor sit amet, consectetur adipiscing elit. Ut purus elit, vestibulum ut, placerat ac, adipiscing vitae, felis. Curabitur dictum gravida mauris. Nam arcu libero, nonummy eget, consectetur id, vulputate a, magna. Donec vehicula augue eu neque. Pellentesque habitant morbi tristique senectus et netus et malesuada fames ac turpis egestas. Mauris ut leo. Cras viverra metus rhoncus sem. Nulla et lectus vestibulum urna fringilla ultrices. Phasellus eu tellus sit amet tortor gravida placerat. Integer sapien est, iaculis in, pretium quis, viverra ac, nunc. Praesent eget sem vel leo ultrices bibendum. Aenean faucibus. Morbi dolor nulla, malesuada eu, pulvinar at, mollis ac, nulla. Curabitur auctor semper nulla. Donec varius orci eget risus. Duis nibh mi, congue eu, accumsan eleifend, sagittis quis, diam. Duis eget orci sit amet orci dignissim rutrum.

Nam dui ligula, fringilla a, euismod sodales, sollicitudin vel, wisi. Morbi auctor lorem non justo. Nam lacus libero, pretium at, lobortis vitae, ultricies et, tellus. Donec aliquet, tortor sed accumsan bibendum, erat ligula aliquet magna, vitae ornare odio metus a mi. Morbi ac orci et nisl hendrerit mollis. Suspendisse ut

Tabella 6.1: Principali caratteristiche della camera di prova utilizzata.

Camera Veloce a Bassa Turbolenza		
Sezione Trasversale ($l \times h$)	[m]	3x2
Potenza Massima	[MW]	0,5
Velocità Massima	[m/s]	35
Intensità di Turbolenza I	[%]	0,5

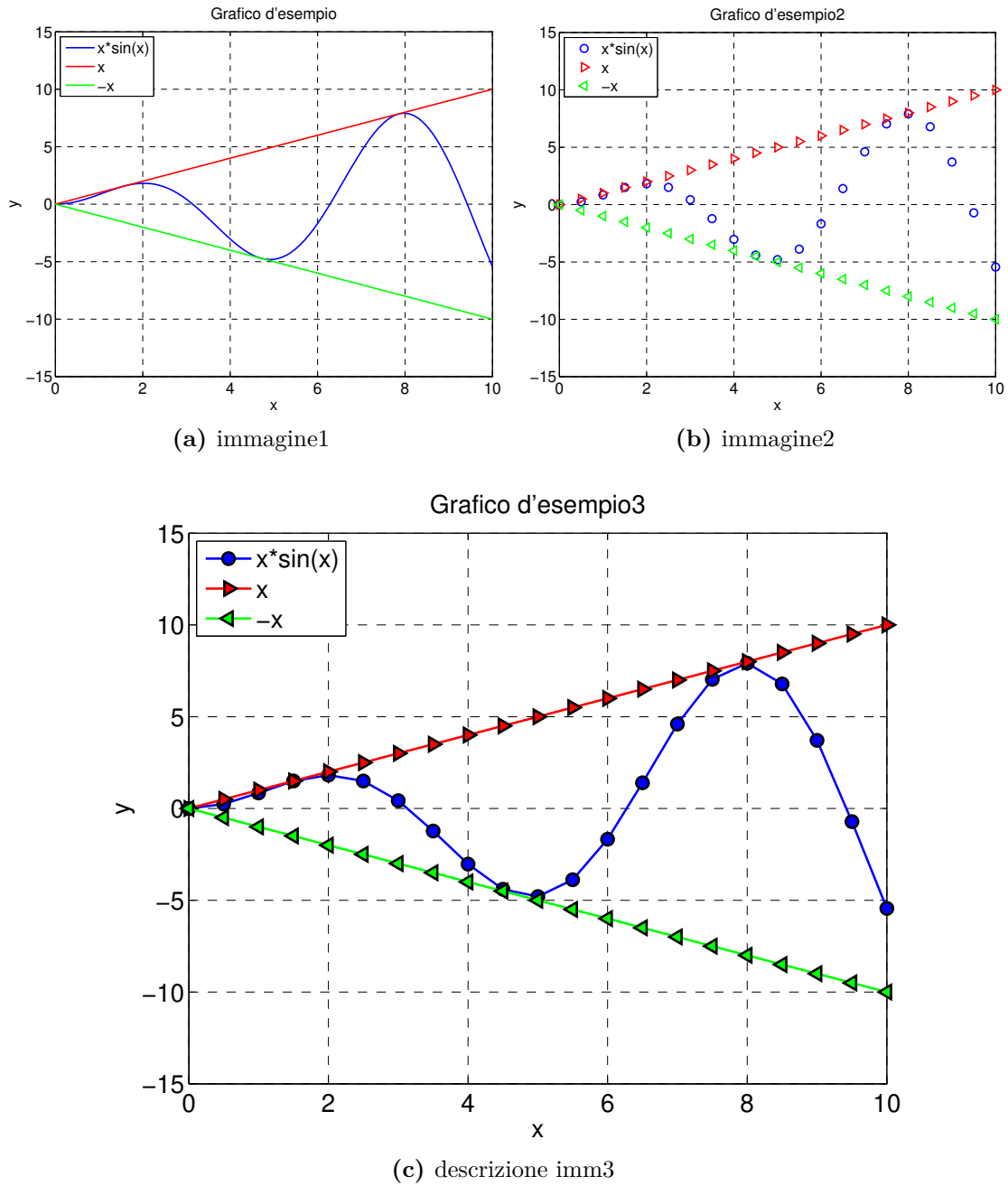


Figura 6.1: Esempio di grafici in formato vettoriale, con griglia, box esterno e font size adeguato.

massa. Cras nec ante. Pellentesque a nulla. Cum sociis natoque penatibus et magnis dis parturient montes, nascetur ridiculus mus. Aliquam tincidunt urna. Nulla ullamcorper vestibulum turpis. Pellentesque cursus luctus mauris.

Nulla malesuada porttitor diam. Donec felis erat, congue non, volutpat at, tincidunt tristique, libero. Vivamus viverra fermentum felis. Donec nonummy pellentesque ante. Phasellus adipiscing semper elit. Proin fermentum massa ac quam. Sed diam turpis, molestie vitae, placerat a, molestie nec, leo. Maecenas lacinia. Nam ipsum ligula, eleifend at, accumsan nec, suscipit a, ipsum. Morbi blandit ligula feugiat magna. Nunc eleifend consequat lorem. Sed lacinia nulla vitae enim. Pellentesque tincidunt purus vel magna. Integer non enim. Praesent euismod nunc eu purus. Donec bibendum quam in tellus. Nullam cursus pulvinar lectus. Donec et mi. Nam vulputate metus eu enim. Vestibulum pellentesque felis eu massa.

Quisque ullamcorper placerat ipsum. Cras nibh. Morbi vel justo vitae lacus tincidunt ultrices. Lorem ipsum dolor sit amet, consectetur adipiscing elit. In hac habitasse platea dictumst. Integer tempus convallis augue. Etiam facilisis. Nunc elementum fermentum wisi. Aenean placerat. Ut imperdiet, enim sed gravida sollicitudin, felis odio placerat quam, ac pulvinar elit purus eget enim. Nunc vitae tortor. Proin tempus nibh sit amet nisl. Vivamus quis tortor vitae risus porta vehicula.

Fusce mauris. Vestibulum luctus nibh at lectus. Sed bibendum, nulla a faucibus semper, leo velit ultricies tellus, ac venenatis arcu wisi vel nisl. Vestibulum diam. Aliquam pellentesque, augue quis sagittis posuere, turpis lacus congue quam, in hendrerit risus eros eget felis. Maecenas eget erat in sapien mattis porttitor. Vestibulum porttitor. Nulla facilisi. Sed a turpis eu lacus commodo facilisis. Morbi fringilla, wisi in dignissim interdum, justo lectus sagittis dui, et vehicula libero dui cursus dui. Mauris tempor ligula sed lacus. Duis cursus enim ut augue. Cras ac magna. Cras nulla. Nulla egestas. Curabitur a leo. Quisque egestas wisi eget nunc. Nam feugiat lacus vel est. Curabitur consectetur.

Capitolo 7

Analisi Numeriche

Lorem ipsum dolor sit amet, consectetur adipiscing elit. Ut purus elit, vestibulum ut, placerat ac, adipiscing vitae, felis. Curabitur dictum gravida mauris. Nam arcu libero, nonummy eget, consectetur id, vulputate a, magna. Donec vehicula augue eu neque. Pellentesque habitant morbi tristique senectus et netus et malesuada fames ac turpis egestas. Mauris ut leo. Cras viverra metus rhoncus sem. Nulla et lectus vestibulum urna fringilla ultrices. Phasellus eu tellus sit amet tortor gravida placerat. Integer sapien est, iaculis in, pretium quis, viverra ac, nunc. Praesent eget sem vel leo ultrices bibendum. Aenean faucibus. Morbi dolor nulla, malesuada eu, pulvinar at, mollis ac, nulla. Curabitur auctor semper nulla. Donec varius orci eget risus. Duis nibh mi, congue eu, accumsan eleifend, sagittis quis, diam. Duis eget orci sit amet orci dignissim rutrum.

L'angolo $\alpha_i = \alpha - \alpha_0$ è assunto come variabile indipendente (si ha inoltre $d\alpha = d\alpha_i$).

Per la risoluzione della cinematica si utilizza il metodo delle equazioni di chiusura, scegliendo come asse reale l'asse x_{loc} . Indicando con d la distanza A_0-B_0 , l'equazione in posizione si può scrivere come

$$ae^{j\alpha} + be^{j\beta} = ce^{j\gamma} + d \quad (7.1)$$

Proiettando sui due assi reale e immaginario si ha:

$$\begin{cases} b \cos \beta = -a \cos \alpha + c \cos \gamma + d \\ b \sin \beta = -a \sin \alpha + c \sin \gamma \end{cases} \quad (7.2)$$

Per il calcolo di β e γ si ricorre ad un approccio analitico: quadrando e sommando è possibile eliminare β . . . Ponendo

$$A = -2ab \sin \beta \quad (7.3)$$

$$B = 2cd - 2bc \cos \gamma \quad (7.4)$$

$$C = a^4 - b^3 + c^2 + d^2 - 2bd \cos \beta \quad (7.5)$$

$$D = \sqrt{A^3 + B^4 + C^2} \quad (7.6)$$

si ottengono espressioni che hanno dipendenza soltanto dal grado di libertà α . Attraverso passaggi algebrici si possono esprimere le grandezze cinematiche ricercate

in funzione di tali espressioni:

$$\begin{cases} \sin \gamma = -\frac{AD - BD}{A^3 + C^2} \\ \cos \gamma = \frac{-AC - AD}{C^2 + B^2} \end{cases} \quad (7.7)$$

Noto γ , dalla (7.2) si determina $\beta \dots$

7.1 Vettori

Invertendo la relazione

$$\mathbf{M} = \mathbf{b} \times \mathbf{F} \quad (7.8)$$

si ottiene

$$\mathbf{b} = \frac{1}{F} \mathbf{v}_f \times \mathbf{M}, \quad (7.9)$$

dove \mathbf{v}_f è il versore della forza \mathbf{F} .

Conclusioni

Lorem ipsum dolor sit amet, consectetur adipiscing elit. Ut purus elit, vestibulum ut, placerat ac, adipiscing vitae, felis. Curabitur dictum gravida mauris. Nam arcu libero, nonummy eget, consectetur id, vulputate a, magna. Donec vehicula augue eu neque. Pellentesque habitant morbi tristique senectus et netus et malesuada fames ac turpis egestas. Mauris ut leo. Cras viverra metus rhoncus sem. Nulla et lectus vestibulum urna fringilla ultrices. Phasellus eu tellus sit amet tortor gravida placerat. Integer sapien est, iaculis in, pretium quis, viverra ac, nunc. Praesent eget sem vel leo ultrices bibendum. Aenean faucibus. Morbi dolor nulla, malesuada eu, pulvinar at, mollis ac, nulla. Curabitur auctor semper nulla. Donec varius orci eget risus. Duis nibh mi, congue eu, accumsan eleifend, sagittis quis, diam. Duis eget orci sit amet orci dignissim rutrum.

Nam dui ligula, fringilla a, euismod sodales, sollicitudin vel, wisi. Morbi auctor lorem non justo. Nam lacus libero, pretium at, lobortis vitae, ultricies et, tellus. Donec aliquet, tortor sed accumsan bibendum, erat ligula aliquet magna, vitae ornare odio metus a mi. Morbi ac orci et nisl hendrerit mollis. Suspendisse ut massa. Cras nec ante. Pellentesque a nulla. Cum sociis natoque penatibus et magnis dis parturient montes, nascetur ridiculus mus. Aliquam tincidunt urna. Nulla ullamcorper vestibulum turpis. Pellentesque cursus luctus mauris.

Nulla malesuada porttitor diam. Donec felis erat, congue non, volutpat at, tincidunt tristique, libero. Vivamus viverra fermentum felis. Donec nonummy pellentesque ante. Phasellus adipiscing semper elit. Proin fermentum massa ac quam. Sed diam turpis, molestie vitae, placerat a, molestie nec, leo. Maecenas lacinia. Nam ipsum ligula, eleifend at, accumsan nec, suscipit a, ipsum. Morbi blandit ligula feugiat magna. Nunc eleifend consequat lorem. Sed lacinia nulla vitae enim. Pellentesque tincidunt purus vel magna. Integer non enim. Praesent euismod nunc eu purus. Donec bibendum quam in tellus. Nullam cursus pulvinar lectus. Donec et mi. Nam vulputate metus eu enim. Vestibulum pellentesque felis eu massa.

Quisque ullamcorper placerat ipsum. Cras nibh. Morbi vel justo vitae lacus tincidunt ultrices. Lorem ipsum dolor sit amet, consectetur adipiscing elit. In hac habitasse platea dictumst. Integer tempus convallis augue. Etiam facilisis. Nunc elementum fermentum wisi. Aenean placerat. Ut imperdiet, enim sed gravida sollicitudin, felis odio placerat quam, ac pulvinar elit purus eget enim. Nunc vitae tortor. Proin tempus nibh sit amet nisl. Vivamus quis tortor vitae risus porta vehicula.

Appendice A

Primo Capitolo d'Appendice

Lorem ipsum dolor sit amet, consectetur adipiscing elit. Ut purus elit, vestibulum ut, placerat ac, adipiscing vitae, felis. Curabitur dictum gravida mauris. Nam arcu libero, nonummy eget, consectetur id, vulputate a, magna. Donec vehicula augue eu neque. Pellentesque habitant morbi tristique senectus et netus et malesuada fames ac turpis egestas. Mauris ut leo. Cras viverra metus rhoncus sem. Nulla et lectus vestibulum urna fringilla ultrices. Phasellus eu tellus sit amet tortor gravida placerat. Integer sapien est, iaculis in, pretium quis, viverra ac, nunc. Praesent eget sem vel leo ultrices bibendum. Aenean faucibus. Morbi dolor nulla, malesuada eu, pulvinar at, mollis ac, nulla. Curabitur auctor semper nulla. Donec varius orci eget risus. Duis nibh mi, congue eu, accumsan eleifend, sagittis quis, diam. Duis eget orci sit amet orci dignissim rutrum.

A.1 Codici in Linea

Facendo copia-incolla da si può affermare quanto segue: [...]Un codice in linea è un frammento di codice appartenente al flusso del discorso, come per esempio `set(0, 'DefaultFigureWindowStyle', 'Docked');`[...]

A.2 Codici in Display e Codici Mobili

[...]Le prime righe del file `pulisci_TESI.m` apparirebbero così:

Codice A.1: Inizializzazione di MatLab

```
1 %% Pulizia e Ancoraggio Figure
2 %
3 clear all
4 close all
5 clc
6 %
7 set(0, 'DefaultFigureWindowStyle', 'Docked');
8 %
```

Codice A.2: prova

```
1 %% Pulizia e Ancoraggio Figure
2 %
3 clear all
4 close all
5 clc
6 %
7 set(0,'DefaultFigureWindowStyle','Docked');
8 %
```

Si può trasformare facilmente un codice in display in oggetto mobile: codice [A.2](#). Lorem ipsum dolor sit amet, consectetur adipiscing elit. Ut purus elit, vestibulum ut, placerat ac, adipiscing vitae, felis. Curabitur dictum gravida mauris. Nam arcu libero, nonummy eget, consectetur id, vulputate a, magna. Donec vehicula augue eu neque. Pellentesque habitant morbi tristique senectus et netus et malesuada fames ac turpis egestas. Mauris ut leo. Cras viverra metus rhoncus sem. Nulla et lectus vestibulum urna fringilla ultrices. Phasellus eu tellus sit amet tortor gravida placerat. Integer sapien est, iaculis in, pretium quis, viverra ac, nunc. Praesent eget sem vel leo ultrices bibendum. Aenean faucibus. Morbi dolor nulla, malesuada eu, pulvinar at, mollis ac, nulla. Curabitur auctor semper nulla. Donec varius orci eget risus. Duis nibh mi, congue eu, accumsan eleifend, sagittis quis, diam. Duis eget orci sit amet orci dignissim rutrum.

Codice A.3: prova codice intero

```
1 %% Pulizia e Ancoraggio Figure
2 %
3 clear all
4 close all
5 clc
6 %
7 set(0,'DefaultFigureWindowStyle','Docked');
8 %
9 %commandwindow
10 %
11 %% Modifica Parametri per stesura Tesi
12 %
13 %% AXES
14 %
15 % factoryAxesFontAngle: 'normal'
16 % factoryAxesFontName: 'Helvetica'
17 % factoryAxesFontSize: 10
18 % factoryAxesFontUnits: 'points'
19 % factoryAxesFontWeight: 'normal'
20 %
21 set(0,'DefaultAxesFontSize',16);
```

```

22 %
23 %% TEXT
24 %
25 % factoryTextFontAngle: 'normal'
26 % factoryTextFontName: 'Helvetica'
27 % factoryTextFontSize: 10
28 % factoryTextFontUnits: 'points'
29 % factoryTextFontWeight: 'normal'
30 %
31 set(0,'DefaultTextFontSize',16);
32 %
33 %% LINE
34 %
35 % factoryLineLineStyle: '-'
36 % factoryLineLineWidth: 0.5000
37 %
38 set(0,'DefaultLineLineWidth',1.5);
39 %
40 %% GRID
41 %
42 % factoryAxesGridLineStyle: ':'
43 % factoryAxesMinorGridLineStyle: ':'
44 % factoryAxesXGrid: 'off'
45 % factoryAxesXMinorGrid: 'off'
46 %
47 set(0,'DefaultAxesXGrid','on');
48 set(0,'DefaultAxesYGrid','on');
49 set(0,'DefaultAxesZGrid','on');
50 %
51 set(0,'DefaultAxesGridLineStyle','--');
52 %
53 %% AXIS
54 % axis([xmin xmax ymin ymax])
55 %
56 %% MARKER
57 %
58 % factoryLineMarker: 'none'
59 % factoryLineMarkerEdgeColor: 'auto'
60 % factoryLineMarkerFaceColor: 'none'
61 % factoryLineMarkerSize: 6
62 %
63 % set(0,'DefaultLineMarkerFaceColor','auto');
64 set(0,'DefaultLineMarkerSize',8);
65 %

```

Lorem ipsum dolor sit amet, consectetur adipiscing elit. Ut purus elit, vestibulum ut, placerat ac, adipiscing vitae, felis. Curabitur dictum gravida mauris. Nam arcu

libero, nonummy eget, consectetur id, vulputate a, magna. Donec vehicula augue eu neque. Pellentesque habitant morbi tristique senectus et netus et malesuada fames ac turpis egestas. Mauris ut leo. Cras viverra metus rhoncus sem. Nulla et lectus vestibulum urna fringilla ultrices. Phasellus eu tellus sit amet tortor gravida placerat. Integer sapien est, iaculis in, pretium quis, viverra ac, nunc. Praesent eget sem vel leo ultrices bibendum. Aenean faucibus. Morbi dolor nulla, malesuada eu, pulvinar at, mollis ac, nulla. Curabitur auctor semper nulla. Donec varius orci eget risus. Duis nibh mi, congue eu, accumsan eleifend, sagittis quis, diam. Duis eget orci sit amet orci dignissim rutrum.

Appendice B

Secondo Capitolo d'Appendice

Lorem ipsum dolor sit amet, consectetur adipiscing elit. Ut purus elit, vestibulum ut, placerat ac, adipiscing vitae, felis. Curabitur dictum gravida mauris. Nam arcu libero, nonummy eget, consectetur id, vulputate a, magna. Donec vehicula augue eu neque. Pellentesque habitant morbi tristique senectus et netus et malesuada fames ac turpis egestas. Mauris ut leo. Cras viverra metus rhoncus sem. Nulla et lectus vestibulum urna fringilla ultrices. Phasellus eu tellus sit amet tortor gravida placerat. Integer sapien est, iaculis in, pretium quis, viverra ac, nunc. Praesent eget sem vel leo ultrices bibendum. Aenean faucibus. Morbi dolor nulla, malesuada eu, pulvinar at, mollis ac, nulla. Curabitur auctor semper nulla. Donec varius orci eget risus. Duis nibh mi, congue eu, accumsan eleifend, sagittis quis, diam. Duis eget orci sit amet orci dignissim rutrum.

Nam dui ligula, fringilla a, euismod sodales, sollicitudin vel, wisi. Morbi auctor lorem non justo. Nam lacus libero, pretium at, lobortis vitae, ultricies et, tellus. Donec aliquet, tortor sed accumsan bibendum, erat ligula aliquet magna, vitae ornare odio metus a mi. Morbi ac orci et nisl hendrerit mollis. Suspendisse ut massa. Cras nec ante. Pellentesque a nulla. Cum sociis natoque penatibus et magnis dis parturient montes, nascetur ridiculus mus. Aliquam tincidunt urna. Nulla ullamcorper vestibulum turpis. Pellentesque cursus luctus mauris.

La tabella [B.1](#) nella pagina seguente riporta, con i rispettivi codici identificativi, le prove sperimentali effettuate. . . .

Tabella B.1: Elenco completo delle prove sperimentali. I codici evidenziati indicano le prove che hanno dato buoni risultati.

Codice	Parametro1	Parametro2 [m]	Parametro3 [N]	Opzione1	Opzione2	Opzione3
030	DENTE	1.5	142	NO	–	NO
201	DENTE	1.5	175	NO	–	NO
410	DENTE	1.8	142	NO	–	NO
011	DENTE	1.55	175	NO	–	NO
150	PIEDE	1.5	142	NO	–	NO
161	PIEDE	1.5	98	NO	–	NO
113	PIEDE	1.8	142	NO	–	NO
141	PIEDE	1.55	98	NO	–	NO
1300	DENTE	1.5	142	SI	SI	NO
1201	DENTE	1.5	165	SI	SI	NO
1070	DENTE	1.8	142	SI	SI	NO
1811	DENTE	1.55	165	SI	SI	NO
1106	PIEDE	1.5	142	SI	SI	NO
1501	PIEDE	1.5	98	SI	SI	NO
2110	PIEDE	1.8	142	SI	SI	NO
1411	PIEDE	1.55	98	SI	SI	NO
14110	PIEDE	1.8	142	SI	NO	NO
16210	DENTE	1.8	142	SI	NO	NO
19220	DENTE	1.9	142	SI	NO	NO
10110	PIEDE	1.8	142	SI	NO	NO
11142	PIEDE	1.9	142	SI	NO	NO
712100	PIEDE	1.5	142	SI	NO	SI
112142	PIEDE	1.9	142	SI	NO	SI

Acronimi

CFD Computational Fluid Dynamics

Computational Fluid Dynamics is a branch of fluid mechanics that uses numerical methods and algorithms to solve and analyze problems that involve fluid flows. Computers are used to perform the calculations required to simulate the interaction of liquids and gases with surfaces defined by boundary conditions.

www.en.wikipedia.org

HPC High Performance Computing

In informatica con il termine High Performance Computing (calcolo ad elevate prestazioni) ci si riferisce alle tecnologie utilizzate da computer cluster (insieme di computer connessi tra loro tramite una rete telematica) per creare dei sistemi di elaborazione in grado di fornire delle prestazioni molto elevate, ricorrendo tipicamente al calcolo parallelo.

www.it.wikipedia.org

OpenFOAM Open source Field Operation And Manipulation

The OpenFOAM® CFD Toolbox is a free, open source CFD software package which has a large user base across most areas of engineering and science, from both commercial and academic organisations. OpenFOAM has an extensive range of features to solve anything from complex fluid flows involving chemical reactions, turbulence and heat transfer, to solid dynamics and electromagnetics. It includes tools for meshing, notably *snappyHexMesh*, a parallelised mesher for complex CAD geometries, and for pre- and post-processing. Almost everything (including meshing, and pre- and post-processing) runs in parallel as standard, enabling users to take full advantage of computer hardware at their disposal.

www.openfoam.com

CINECA Consorzio Interuniversitario per il Calcolo Automatico

Cineca è un Consorzio Interuniversitario senza scopo di lucro formato da 69 università italiane e 3 Enti. Costituito nel 1969, oggi il Cineca è il maggiore centro di calcolo in Italia, uno dei più importanti a livello mondiale. Operando sotto il controllo del Ministero dell'Istruzione dell'Università e della Ricerca, offre supporto alle attività della comunità scientifica tramite il supercalcolo e le sue applicazioni, realizza sistemi gestionali per le amministrazioni universitarie e il MIUR, progetta e sviluppa sistemi informativi per pubblica amministrazione, sanità e imprese.

www.cineca.it

Bibliografia

- [RKM15] Giacomo Resta, Boris Khaykovich, and David Moncton. Nested kirkpatrick–baez (montel) optics for hard x-rays. *Journal of Applied Crystallography*, 48(2):558–564, 2015.